



Available online at [www.sciencedirect.com](http://www.sciencedirect.com)



Franklin Institute 00 (2023) 1–21



# Real-Time Control of a Quadrotor Experimental Platform using Linear Quadratic Integral Differential Game

Hadi Nobahari

*Department of Aerospace Engineering Sharif University of Technology Tehran, Iran*

Ali BaniAsad

*Department of Aerospace Engineering Sharif University of Technology Tehran, Iran*

Reza Pordal

*Department of Aerospace Engineering Sharif University of Technology Tehran, Iran*

Alireza Sharifi

*Department of Aerospace Engineering Sharif University of Technology Tehran, Iran*

---

## Abstract

This research paper presents a novel approach to quadrotor attitude control that draws on differential game theory. The approach uses a linear quadratic Gaussian (LQG) controller with integral actions. Accurate attitude control is of utmost importance for safe and effective quadrotor flight, particularly in the presence of disturbances. To develop a dependable and effective control system, the motion equations with nonlinearity for the quadrotor's experimental setup are transformed into a continuous-time state-space model through linearization. Experimental data are used to identify model parameters, and attitude control commands are determined using two-player approaches. By mini-maximizing a quadratic set of criteria, which is the total of the outputs and disturbances weighted by the amount of control effort, one player minimizes the command while the other generates disturbances. The performance of the proposed approach is evaluated by comparing it to a linear quadratic regulator controller in level flight. The results demonstrate that the proposed approach effectively dissipates disturbances and outperforms linear quadratic regulator controllers, thereby contributing to the development of robust and effective attitude control systems for quadrotors.

© 2011 Published by Elsevier Ltd.

**Keywords:**

Linear quadratic Gaussian controller, Differential game theory, Quadrotor, Continuous state-space model, 3-degree-of-freedom experimental platform, Attitude Control Optimization, Robust disturbance rejection.

---

## 1. Introduction

The investigation, strategic operations, optical sensing, entertainment, and farming are all used by quadrotors in today's society [1]. Various subsystems of the quadrotor control system are responsible for the quadrotor's perfor-

---

*Email addresses:* nobahari@sharif.edu (Hadi Nobahari), ali.baniasad@ae.sharif.edu (Ali BaniAsad), email address (Reza Pordal), alireza\_sharifi@ae.sharif.edu (Alireza Sharifi)

mance, including attitude, altitude, and position. Maintaining the desired attitude outputs is essential for quadrotor attitude control, particularly in the presence of sudden disturbances. This can be achieved by controlling the rotor rotational speeds[2]. Consequently, there is a growing body of research focusing on the development of automatic control strategies for quadrotors to effectively manage disturbances and maintain desired attitudes. The quadrotor attitude is controlled by a Proportional Integral Derivative (PID) controller in [3, 4]. During disturbances, however, this controller has not effectively achieved the control objectives. Model-based approaches to controller design are utilized to resolve this issue [5, 6]. Quadrotor attitude models and disturbances determine the direction of the best control commands using these controllers.

The literature has proposed numerous models-based controllers to provide a faster control algorithm when dealing with modeling errors and reducing disturbances. An intelligent controller, a robust controller, a nonlinear controller, and an optimal controller are some of these types of controllers.

Various control approaches based on intelligent logic, such as machine learning [7], evolutionary computation [8], iterative learning [9], reinforcement learning [10], and fuzzy logic [11], have been extensively employed for quadrotor attitude regulation. Numerous nonlinear control techniques have been proposed to regulate orientation angles of quadrotors, including Synergetic Control [12], Sliding Mode Control (SMC) [13], and Feedback Linearization (FBL) [14]. Robust control methods such as  $H_\infty$  [15, 16] and  $\mu$ -synthesis [17] have also been utilized to stabilize the attitudes of quadrotors under conditions of extreme uncertainty and worst-case scenarios. Quadrotors have also been controlled using optimal controllers, such as the Linear Quadratic Gaussian (LQG) [18] and the Linear Quadratic Regulator (LQR) [19]. Optimizing feedback gains is achieved by utilizing both regulation and control effort to minimize a quadratic criterion. The Linear Quadratic Regulator Differential Game (LQR-DG) is a robust and optimal control strategy that has been extensively utilized in controlling various nonlinear and complex systems, including quadrotors. This approach employs a linear system model to control its outputs while minimizing a cost function through mini-maximization. The LQR-DG approach has been demonstrated to offer excellent regulation performance and control effort while being robust to external disturbances. For instance, it has been successfully applied to control a ship controller, showcasing its effectiveness and versatility in handling complex control problems [20, 21]. By means of an analytical pursuit-evasion process, the LQR-DG control approach generates precise and optimized control commands. This unique feature sets the LQR-DG controller apart from other conventional optimal control techniques and enables one player to track the most appropriate control command while the other creates disturbances.

This study proposes a new controller for quadrotors based on the LQG technique with integral action, using differential game theory to optimize control performance in the presence of disturbance. Attitude control in the presence of disturbance is essential for ensuring safe and effective quadrotor flight. In order to devise this control approach, a continuous state-space model for a quadrotor's experimental setup is formulated by linearizing the system's equations of motion, which are inherently nonlinear, and identifying its parameters based on experimental data. This approach involves transforming the nonlinear dynamics into a linear system that can be analyzed more readily. The proposed Linear Quadratic Regulator Differential Game (LQR-DG) controller offers an optimal control strategy for generating efficient control commands for quadrotors. The approach employs a two-player system, wherein one player optimizes the command while the other creates disturbances through mini-maximization of a quadratic criterion. This technique not only ensures efficient control but also offers a robust and versatile approach to handle complex control problems. The proposed approach is evaluated against a linear quadratic regulator controller in level flight. The results show that the LQIG-DG controller effectively dissipates disturbances and outperforms the linear quadratic regulator controller. This study presents an important contribution to the development of robust and effective attitude control systems for quadrotors.

The following sections of this research paper provide a comprehensive analysis of the proposed control approach. Section 2 defines detailed derivations of the dynamics model and quadrotor's experimental platform, respectively. Section 4 explicates the proposed LQIG-DG controller architecture. The effectiveness of the controller is assessed in section 5, which is followed by the conclusion in section 6.

## 2. Problem Statement

A complex nonlinear system describes the experimental platform of the quadrotor depicted in Figure 1. During its rotation, the quadrotor can adjust its pitch, roll, and yaw angles. An Inertial Measurement Unit (IMU) is used to measure the acceleration and rotational velocities along the three orthogonal axes, which are affected by noise. To

estimate the states of the quadrotor, including its angular velocities and Euler angles, a nonlinear filter is utilized. A graphical representation of the LQIG-DG controller structure is depicted in Figure 2. The estimated states allow for the stabilization of the quadrotor setup.



Figure 1: 3DoF setup of the quadrotor.

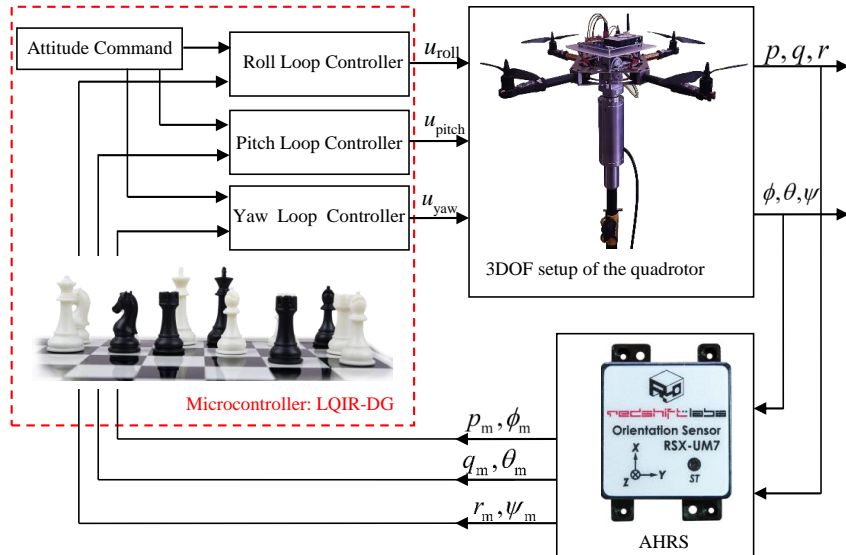


Figure 2: Structure of the LQIG-DG Controller Illustrated in a Block Diagram.

### 3. Dynamic Model of the Quadrotor Platform

In this section, first, a nonlinear model for the quadrotor platform is derived. Then, a state-space model and a linear model are developed for control purposes to be utilized in a controller strategy. Finally, a linear identification method is applied to identify the parameters of the quadrotor

### 3.1. Quadrotor Configuration

Figure 3 illustrates the quadrotor schematic, depicting four rotors with rotational velocity  $\Omega_r$  rotating around the  $z_B$  axis in the coordinate system of body. The rotational direction of Rotor 1 and Rotor 3 in the counterclockwise direction counteracts the yawing moment, whereas the clockwise rotation of Rotors 2 and 4 counteracts the yawing moment.

Figure 3 shows the quadrotor schematic. It depicts four rotors rotating around the  $z_B$  axis in the coordinate system of the body. The rotors have a rotational velocity of  $\Omega_r$ . The quadrotor platform has 3 degrees of freedom, including roll, pitch, and yaw motions, which are described by roll ( $\phi$ ), pitch ( $\theta$ ), and yaw ( $\psi$ ) angles, respectively. The counterclockwise rotation of Rotors 1 and 3 generates a moment that counteracts the yawing moment, while the clockwise rotation of Rotors 2 and 4 produces a moment that also counteracts the yawing moment.

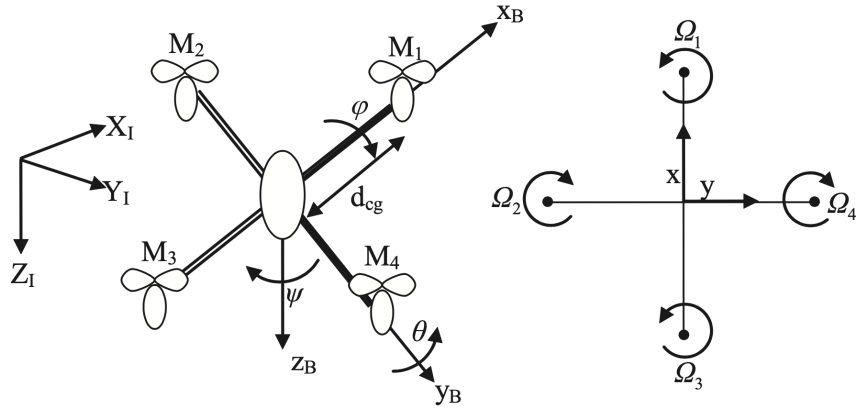


Figure 3: Quadrotor Configuration.

### 3.2. Dynamic Modeling of the Quadrotor Platform

Here, according to Newton-Euler, the dynamic model of the quadrotor platform is derived as follows [22, 23]:

$$\dot{p} = \frac{I_{yy} - I_{zz}}{I_{xx}} qr + q \frac{I_{rotor}}{I_{xx}} \Omega_r + \frac{u_{roll}}{I_{xx}} + \frac{d_{roll}}{I_{xx}} \quad (1)$$

$$\dot{q} = \frac{I_{zz} - I_{xx}}{I_{yy}} rp + p \frac{I_{rotor}}{I_{xx}} \Omega_r + \frac{u_{pitch}}{I_{yy}} + \frac{d_{pitch}}{I_{yy}} \quad (2)$$

$$\dot{r} = \frac{I_{xx} - I_{yy}}{I_{zz}} pq + \frac{u_{yaw}}{I_{zz}} + \frac{d_{yaw}}{I_{zz}} \quad (3)$$

The  $(p, q, r)$  represent the rotational variables, and  $d_{roll}$ ,  $d_{pitch}$ , and  $d_{yaw}$  denote the disturbances produced in the  $x_B$ ,  $y_B$ , and  $z_B$  axes, respectively. Additionally,  $I_{xx}$ ,  $I_{yy}$ , and  $I_{zz}$  are the principal moments of inertia, and  $I_{rotor}$  is the rotor inertia about its axis. Euler angle rates are also determined from angular body rates as follows:

$$\begin{bmatrix} \dot{\phi} \\ \dot{\theta} \\ \dot{\psi} \end{bmatrix} = \begin{bmatrix} 1 & \sin(\phi) \tan(\theta) & \cos(\phi) \tan(\theta) \\ 0 & \cos(\phi) & -\sin(\phi) \\ 0 & \sin(\phi)/\cos(\theta) & \cos(\phi)/\cos(\theta) \end{bmatrix} \begin{bmatrix} p \\ q \\ r \end{bmatrix} \quad (4)$$

The residual rotor velocity, denoted by  $\Omega_r$ , is calculated as follows:

$$\Omega_r = -\Omega_1 + \Omega_2 - \Omega_3 + \Omega_4 \quad (5)$$

### 3.3. Innovative Control Strategies for Quadrotor

The control inputs  $u_{\text{roll}}$ ,  $u_{\text{pitch}}$ , and  $u_{\text{yaw}}$  are to the moments generated by the quadrotor's rotors along the roll, pitch, and yaw axes, respectively, and are defined as follows:

$$u_{\text{roll}} = b d_{\text{cg}} (\Omega_2^2 - \Omega_4^2) \quad (6)$$

$$u_{\text{pitch}} = b d_{\text{cg}} (\Omega_1^2 - \Omega_3^2) \quad (7)$$

$$u_{\text{yaw}} = d (\Omega_1^2 - \Omega_2^2 + \Omega_3^2 - \Omega_4^2) \quad (8)$$

where  $d_{\text{cg}}$ ,  $d$ , and  $b$  represent the distance between the rotors and the gravity center, drag factor, and thrust factor, respectively. The rotational velocity commands are computed as follows:

$$\Omega_{c,1}^2 = \Omega_{\text{mean}}^2 + \frac{1}{2b d_{\text{cg}}} u_{\text{pitch}} + \frac{1}{4d} u_{\text{yaw}} \quad (9)$$

$$\Omega_{c,2}^2 = \Omega_{\text{mean}}^2 + \frac{1}{2b d_{\text{cg}}} u_{\text{roll}} - \frac{1}{4d} u_{\text{yaw}} \quad (10)$$

$$\Omega_{c,3}^2 = \Omega_{\text{mean}}^2 - \frac{1}{2b d_{\text{cg}}} u_{\text{pitch}} + \frac{1}{4d} u_{\text{yaw}} \quad (11)$$

$$\Omega_{c,4}^2 = \Omega_{\text{mean}}^2 - \frac{1}{2b d_{\text{cg}}} u_{\text{roll}} - \frac{1}{4d} u_{\text{yaw}} \quad (12)$$

In the above equation,  $\Omega_{\text{mean}}$  is nominal rotational velocities of the rotors.

### 3.4. State-Space Formulation

Here, by defining  $x_1 = p$ ,  $x_2 = q$ ,  $x_3 = r$ ,  $x_4 = \phi$ ,  $x_5 = \theta$ , and  $x_6 = \psi$ , the formulation of the quadrotor platform is presented as follows:

$$\dot{x}_1 = \Gamma_1 x_2 x_3 + \Gamma_2 x_2 \Omega_r + \Gamma_3 u_{\text{roll}} + \Gamma_3 d_{\text{roll}} \quad (13)$$

$$\dot{x}_2 = \Gamma_4 x_1 x_3 - \Gamma_5 x_1 \Omega_r + \Gamma_6 u_{\text{pitch}} + \Gamma_6 d_{\text{pitch}} \quad (14)$$

$$\dot{x}_3 = \Gamma_7 x_1 x_2 + \Gamma_8 u_{\text{yaw}} + \Gamma_8 d_{\text{yaw}} \quad (15)$$

$$\dot{x}_4 = x_1 + (x_2 \sin(x_4) + x_3 \cos(x_4)) \tan(x_5) \quad (16)$$

$$\dot{x}_5 = x_2 \cos(x_4) - x_3 \sin(x_4) \quad (17)$$

$$\dot{x}_6 = (x_2 \sin(x_4) + x_3 \cos(x_4)) / \cos(x_5) \quad (18)$$

where  $\Gamma_i (i = 1, \dots, 8)$  is defined as follows:

$$\begin{aligned} \Gamma_1 &= \frac{I_{yy} - I_{zz}}{I_{xx}}, & \Gamma_2 &= \frac{I_{\text{rotor}}}{I_{xx}}, & \Gamma_3 &= \frac{1}{I_{xx}} \\ \Gamma_4 &= \frac{I_{zz} - I_{xx}}{I_{yy}}, & \Gamma_5 &= \frac{I_{\text{rotor}}}{I_{xx}}, & \Gamma_6 &= \frac{1}{I_{yy}} \\ \Gamma_7 &= \frac{I_{xx} - I_{yy}}{I_{zz}}, & \Gamma_8 &= \frac{1}{I_{zz}} \end{aligned} \quad (19)$$

Moreover, the measurement vector, obtained from the AHRS sensor is presented as follows:

$$\mathbf{z} = [p \ q \ r \ \phi \ \theta \ \psi]^T \quad (20)$$

In the above equation, the superscripts T indicate the transpose notation.

### 3.5. Linear Model

The linear continuous-time model of the quadrotor platform equilibrium points ( $\mathbf{x}_e = 0$  and  $\mathbf{u}_e = 0$ ) is represented as:

$$\dot{\mathbf{x}}(t) = \mathbf{A} \mathbf{x}(t) + \mathbf{B} \mathbf{u}(t) + \mathbf{B}_d \mathbf{d}(t) \quad (21)$$

where  $\dot{\mathbf{x}} = [\dot{x}_{\text{roll}} \quad \dot{x}_{\text{pitch}} \quad \dot{x}_{\text{yaw}}]$ , defined as:

$$\mathbf{x}_{\text{roll}} = \begin{bmatrix} p \\ \phi \end{bmatrix}, \quad \mathbf{x}_{\text{pitch}} = \begin{bmatrix} q \\ \theta \end{bmatrix}, \quad \mathbf{x}_{\text{yaw}} = \begin{bmatrix} r \\ \psi \end{bmatrix} \quad (22)$$

where  $\mathbf{A}$  is the dynamic system matrix, denoted

$$\mathbf{A} = \begin{bmatrix} \mathbf{A}_{\text{roll}} & \mathbf{0} & \mathbf{0} \\ \mathbf{0} & \mathbf{A}_{\text{pitch}} & \mathbf{0} \\ \mathbf{0} & \mathbf{0} & \mathbf{A}_{\text{yaw}} \end{bmatrix} \quad (23)$$

Moreover,  $\mathbf{B}$  and  $\mathbf{B}_d$  are the input and disturbance matrices, defined as:

$$\mathbf{B} = \mathbf{B}_d = \begin{bmatrix} \mathbf{B}_{\text{roll}} & \mathbf{0} & \mathbf{0} \\ \mathbf{0} & \mathbf{B}_{\text{pitch}} & \mathbf{0} \\ \mathbf{0} & \mathbf{0} & \mathbf{B}_{\text{yaw}} \end{bmatrix} \quad (24)$$

In addition, the input matrices and state are shown as

$$\mathbf{A}_{\text{roll}} = \mathbf{A}_{\text{pitch}} = \mathbf{A}_{\text{yaw}} = \begin{bmatrix} 0 & 0 \\ 1 & 0 \end{bmatrix} \quad (25)$$

$$\mathbf{B}_{\text{roll}} = \begin{bmatrix} 1 \\ \frac{1}{I_{xx}} \\ 0 \end{bmatrix}; \quad \mathbf{B}_{\text{pitch}} = \begin{bmatrix} 1 \\ \frac{1}{I_{yy}} \\ 0 \end{bmatrix}; \quad \mathbf{B}_{\text{yaw}} = \begin{bmatrix} 1 \\ \frac{1}{I_{zz}} \\ 0 \end{bmatrix} \quad (26)$$

### 3.6. Identification of the Platform Parameters

This section the Nonlinear Least Squares (NLS) algorithm is utilized for estimating the model parameter ( $\Gamma$ ) of the 3DoF experimental platform using the experimental data. This technique is based on the Trust-Region Reflective Least Squares (TRRLS) method to the iteratively find the values of the model parameters based on the minimization of a cost function, defined as follows:

$$\min_{\Gamma_i} (\| e(\Gamma_i) \|^2) = \min_{\Gamma_i} \left( \sum_{j=1}^n (\mathbf{z}_j - \hat{\mathbf{z}}_j)(\mathbf{z}_j - \hat{\mathbf{z}}_j)^T \right) \quad (27)$$

where  $\mathbf{z}$  and  $\hat{\mathbf{z}}$  are the experimental and simulated output signals, when the same input signals are applied ones.

The optimization process involves finding a vector  $\mathbf{\Gamma}$  by iteratively updating the values of the model parameters until convergence is achieved. The structure of the proposed identification approach is illustrate in figure 4

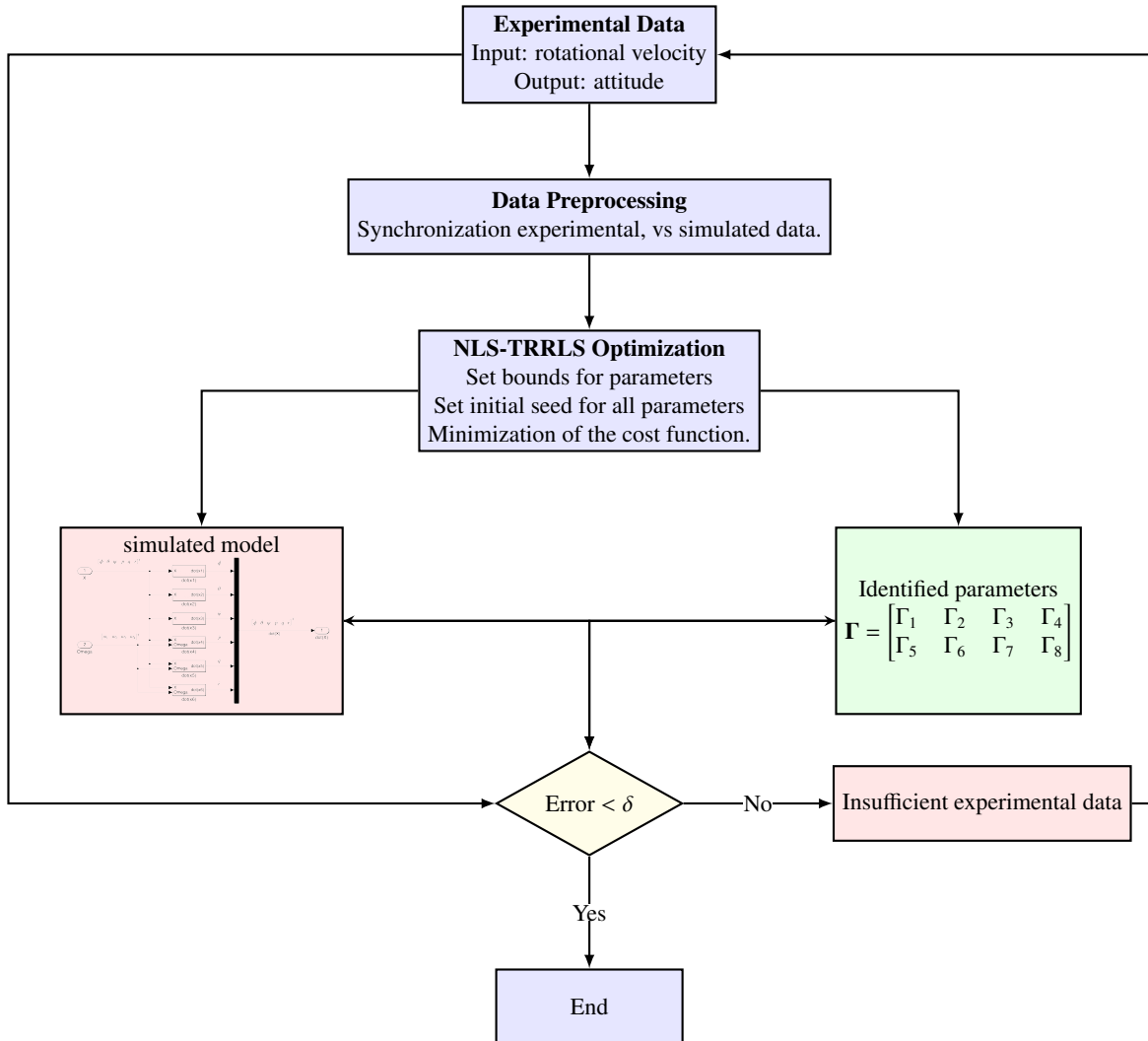


Figure 4: Structure of TRRLS identification approach.

#### 4. Formulation of the LQDG Controller

Here, the LQR-DG controller is augmented with an integral action to eliminate steady-state errors. For this purpose, the augmented states of the quadrotor platform, including states and their integrals, are selected. The design methodology of the LQR-DG controller is introduced to generate optimal control signals for the three degrees of freedom platform.

##### 4.1. Augmented State Space Development

To integrate the integrator into the control strategy architecture, the augmented state variables are defined as below:

$$\mathbf{x}_{\mathbf{a}_i} = \begin{bmatrix} \mathbf{x}_i \\ \int \mathbf{x}_i \end{bmatrix} \quad (28)$$

The dynamics model of the quadrotor, as expressed by Eq. (21), is reformulated into an augmented state-space model that incorporates the roll ( $\phi$ ), pitch ( $\theta$ ), and yaw ( $\psi$ ) angles. The augmented state-space model provides a

comprehensive description of the quadrotor's dynamic behavior, enabling the design of effective control strategies. The ensuing state-space model that integrates the augmented state variables is mathematically represented defined in the following manner:

$$\dot{\mathbf{x}}_a(t) = \mathbf{A}_a \mathbf{x}_a(t) + \mathbf{B}_a \mathbf{u}(t) + \mathbf{B}_{d_a} \mathbf{d}(t) \quad (29)$$

$\mathbf{B}_a$  and  $\mathbf{A}_a$ , which are expressed as below :

$$\mathbf{B}_a = \mathbf{B}_{d_a} = \begin{bmatrix} \mathbf{B} \\ \mathbf{0} \end{bmatrix} \quad (30)$$

$$\mathbf{A}_a = \begin{bmatrix} \mathbf{A} & \mathbf{0} \\ \mathbf{I} & \mathbf{0} \end{bmatrix} \quad (31)$$

In the aforementioned expression, the notation  $\mathbf{I}$  denotes the identity matrix.

#### 4.2. LQR-DG Control Scheme with Integral Action

In accordance with the principles of differential game theory, the LQIR-DG controller is designed to be robust and optimal. In the LQIR-DG scheme, two fundamental players are selected, one for determining the control command and the other for generating the worst possible disturbance. The primary player must minimize the following cost function to achieve the primary objective, while the other player must maximize it:

$$\min_u \max_d J(\mathbf{x}_{a_i}, d_i, u_i) = J(\mathbf{x}_{a_i}, u_i^*, d_i^*) = \min_d \max_u \int_0^{t_f} \left( \mathbf{x}_{a_i}^T \mathbf{Q}_i \mathbf{x}_{a_i} + u_i^T R u_i - d_i^T R_d d_i \right) dt \quad (32)$$

where  $\mathbf{Q}_i$ ,  $R_d$ , and  $R$  are weight coefficients of the function. The final time is denoted by  $t_f$ . By solving the above problem, the control command is computed as follows [24]:

$$d_i(t) = \mathbf{K}_{d_i}(t) \mathbf{x}_{a_i}(t) \quad (33)$$

Moreover, the worst disturbance is obtained as:

$$u_i(t) = -\mathbf{K}_i(t) \mathbf{x}_{a_i}(t) \quad (34)$$

where  $\mathbf{K}_{d_i}$  and  $\mathbf{K}_i$  are gain values that change over time and are defined as follows:

$$\mathbf{K}_i = R^{-1} \mathbf{B}_{a_i}^T \mathbf{P}_{a_i}(t) \quad (35)$$

$$\mathbf{K}_{d_i} = R_d^{-1} \mathbf{B}_{a_{d_i}}^T \mathbf{P}_{a_{d_i}}(t) \quad (36)$$

where  $\mathbf{P}_{a_i}(t)$  and  $\mathbf{P}_{a_{d_i}}(t)$  satisfy

$$\dot{\mathbf{P}}_{a_{d_i}}(t) = -\mathbf{A}_a^T \mathbf{P}_{a_{d_i}}(t) - \mathbf{Q}_i - \mathbf{P}_{a_{d_i}}(t) \mathbf{A}_a + \mathbf{P}_{a_{d_i}}(t) \mathbf{S}_{a_i}(t) \mathbf{P}_{a_i}(t) + \mathbf{P}_{a_{d_i}}(t) \mathbf{S}_{a_{d_i}}(t) \mathbf{P}_{a_{d_i}}(t) \quad (37)$$

$$\dot{\mathbf{P}}_{a_i}(t) = -\mathbf{A}_a^T \mathbf{P}_{a_i}(t) - \mathbf{Q}_i - \mathbf{P}_{a_i}(t) \mathbf{A}_a + \mathbf{P}_{a_i}(t) \mathbf{S}_{a_{d_i}}(t) \mathbf{P}_{a_{d_i}}(t) + \mathbf{P}_{a_i}(t) \mathbf{S}_{a_i}(t) \mathbf{P}_{a_i}(t) \quad (38)$$

In this study, the feedback control law is developed using the asymptotic behavior of the equations as  $t_f$  approaches infinity. The matrices  $\mathbf{S}_{a_i}$  and  $\mathbf{S}_{a_{d_i}}$  are determined by utilizing the matrices  $\mathbf{B}_{a_i}$  and  $\mathbf{B}_{a_{d_i}}$  along with the symmetric nonnegative definite matrices  $R$  and  $R_d$ . Specifically,  $\mathbf{S}_{a_i}$  is defined as  $\mathbf{B}_{a_i} R^{-1} \mathbf{B}_{a_i}^T$ , while  $\mathbf{S}_{a_{d_i}}$  is defined as  $\mathbf{B}_{a_{d_i}} R_d^{-1} \mathbf{B}_{a_{d_i}}^T$ .

## 5. Experimental Findings and Analysis

The current study presents an investigation of the effectiveness of the LQIR-DG control approach in the regulation of an experimental quadrotor platform's roll, pitch, and yaw movements. Numerical simulations are used to tune the parameters of the controller to achieve optimal and resilient performance. The comparative performance analysis of the LQIR-DG controller is carried out with respect to other control strategies, namely LQR, PID, and LQIR. The quadrotor's parameters are listed in Table 1.

Furthermore, the weighting coefficients of the LQIR-DG controller are provided in Table 2.

Table 1: Quadrotor Parameters

Parameter	Value	Unit
$d_{cg}$	0.2	m
$d$	$3.2 \times 10^{-6}$	N.m.sec <sup>2</sup> /rad <sup>2</sup>
$b$	$3.13 \times 10^{-5}$	N.sec <sup>2</sup> /rad <sup>2</sup>
$I_{xx}$	0.02839	kg.m <sup>2</sup>
$I_{yy}$	0.03066	kg.m <sup>2</sup>
$I_{zz}$	0.0439	kg.m <sup>2</sup>
$I_{rotor}$	$4.4398 \times 10^{-5}$	kg.m <sup>2</sup>
$\Omega_{mean}$	3000	rpm

Table 2: LQIR-DG Controller Parameters

Control Channel	Weighting Matrix	Matrix Values
Roll	$Q_{roll}$	diag([0.02, 65.96, 83.04, 0.00])
Pitch	$Q_{pitch}$	diag([435.01, 262.60, 262.60, 0.00])
Yaw	$Q_{yaw}$	diag([ $4 \times 10^{-4}$ , 0.00, 0.133, 0])
$R$		1
$R_d$		1.2764

### 5.1. Identification of the 3DoF experimental setup model

As described in Section 3.4, the parameters of the quadrotor setup, denoted by  $\Gamma_i (i = 1, \dots, 8)$ , must be identified using the NRS algorithm. The NLS-TRRLS algorithm is implemented in Matlab R2022b® to increase the accuracy of parameter identification. Three scenarios, as outlined in Table 3, are considered to ensure comprehensive parameter identification. When the stopping condition of the NLS algorithm is met, the optimal values of the quadrotor parameters are computed and presented in Table 4. The intelligent movement of the parameters during the optimization process is illustrated in Figure 4.

In the first scenario, shown in Figure 5, the quadrotor is rotated about only one axis (roll, pitch, or yaw axes) to identify the parameters  $\Gamma_3$ ,  $\Gamma_6$ , and  $\Gamma_8$ . In the second scenario, as illustrated in Figure 6, the parameters  $\Gamma_2$  and  $\Gamma_5$  are estimated by allowing the experimental setup to freely rotate around its roll and pitch axes. Finally, in the last scenario, depicted in Figure 7, the parameters  $\Gamma_1$ ,  $\Gamma_4$ , and  $\Gamma_7$  of the UAV model are identified by rotating the quadrotor setup around three axes. These results confirm the consistency between the outputs of the simulation results for the quadrotor model and the actual experimental setup.

Table 3: Scenarios for identification of quadrotor model.

<b>Scenario</b>	<b>Description</b>	<b>Initial Conditions</b>		<b>angular velocity Commands</b>			
I	Roll free	38		2000 2000 2000 3400			
	Pitch free	-15		3700 2000 2000 2000			
	Yaw free	-75		2000 3300 2000 3300			
II	Roll and Pitch free	8	-5	1700	3800	2400	1700
III	Roll, Pitch, and Yaw free	8	-3	-146	1700	3800	2400
					1700		

Table 4: True values of the quadrotor parameters.

<b>Parameter</b>	<b>Value</b>	<b>Parameter</b>	<b>Value</b>
$\Gamma_1$	-0.9622	$\Gamma_5$	$3.6441 \times 10^{-4}$
$\Gamma_2$	-0.0154	$\Gamma_6$	$7.5395 \times 10^{-5}$
$\Gamma_3$	$5.4716 \times 10^{-5}$	$\Gamma_7$	0.1308
$\Gamma_4$	1.0457	$\Gamma_8$	$4.3753 \times 10^{-5}$

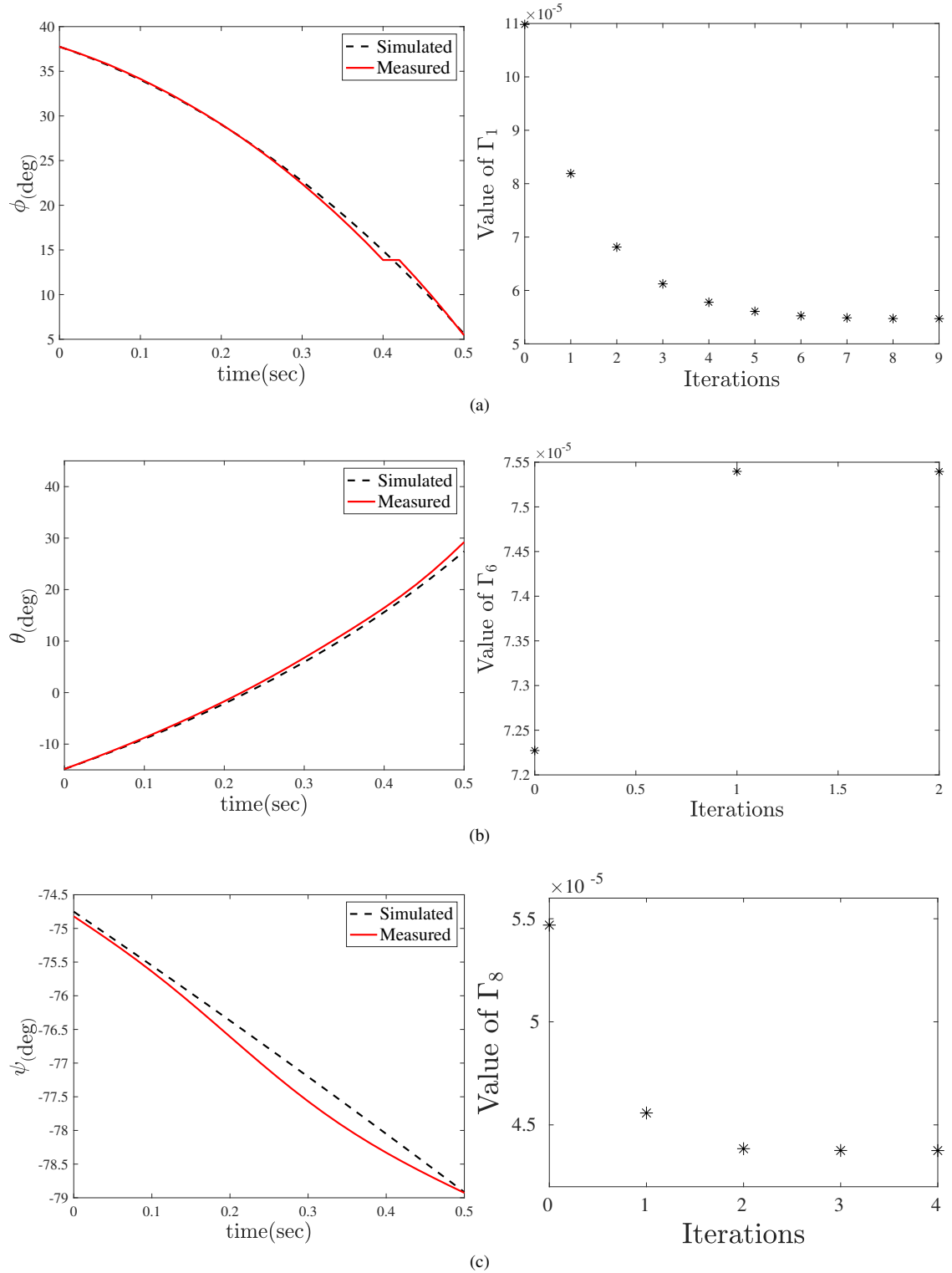


Figure 5: Identification process results when the quadrotor rotates about only one axis: (a) Identification of  $\Gamma_3$  in free roll. (b) Identification of  $\Gamma_6$  in free pitch. (c) Identification of  $\Gamma_8$  in free yaw.

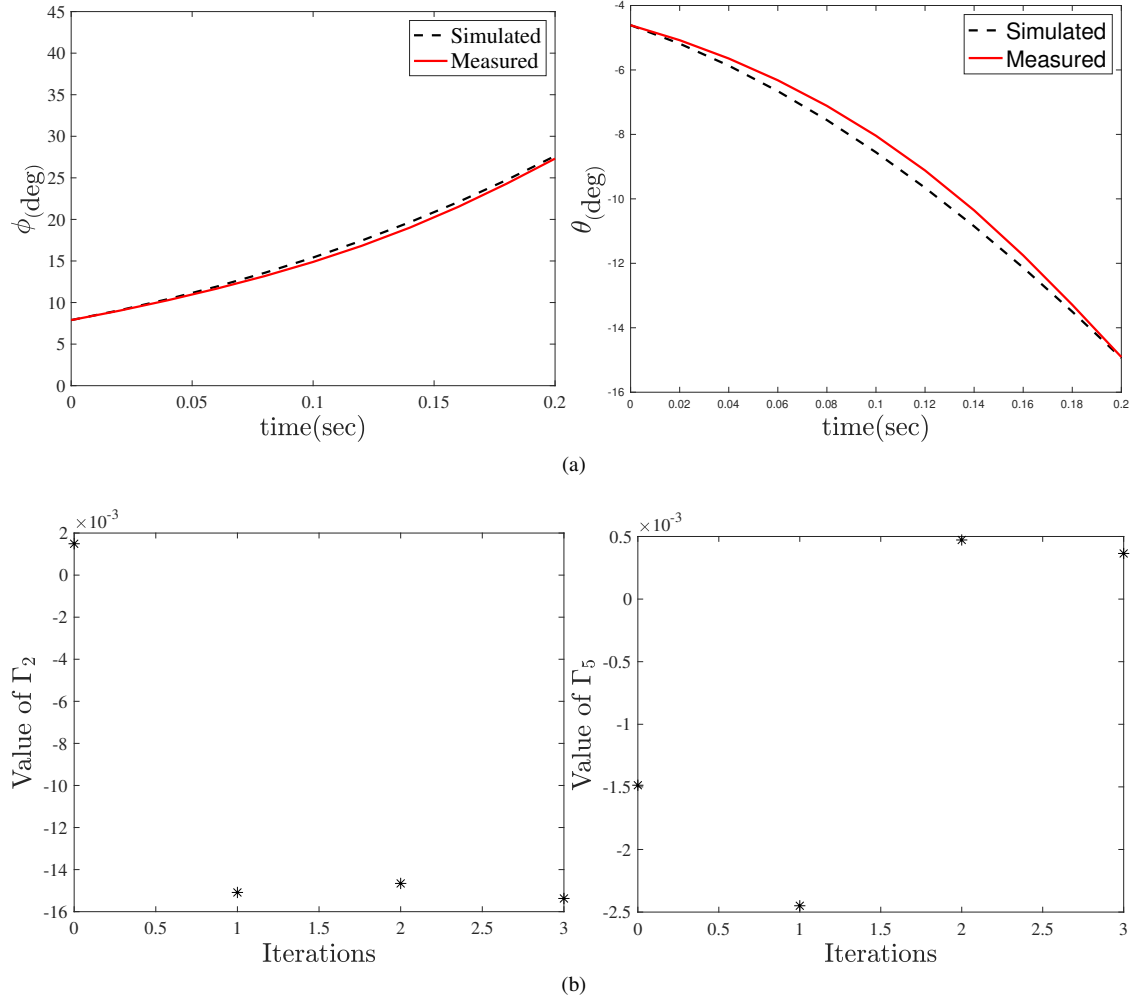


Figure 6: Identification process results when the quadrotor rotates about its roll and pitch axes: (a) Comparison of Simulation and experimental results. (b) Identification of  $\Gamma_2$  and  $\Gamma_5$ .

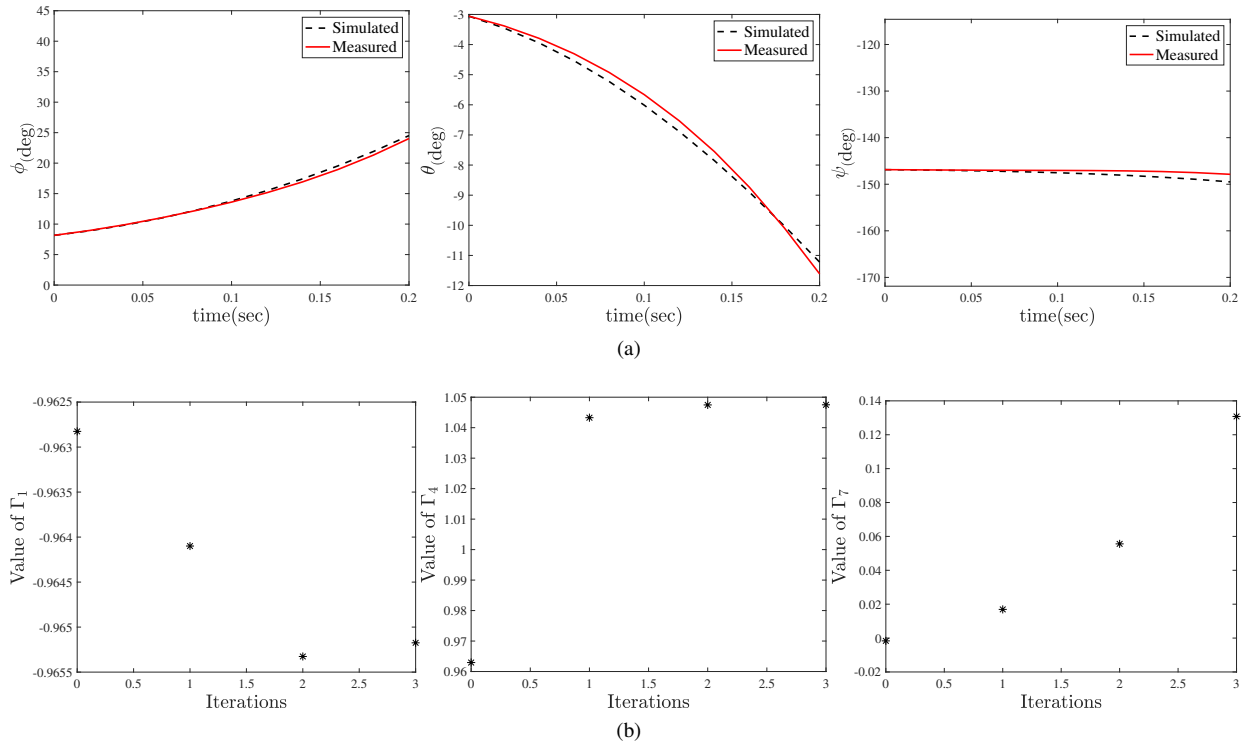


Figure 7: Identification process results when the quadrotor rotates about its roll, pitch, and yaw axes: (a) Comparison of Simulation and experimental results. (b) Identification of  $\Gamma_1$ ,  $\Gamma_4$  and  $\Gamma_7$  parameters.

### 5.2. Assessment of LQIR-DG Control Strategy

The performance of the LQIR-DG control strategy is assessed in three aspects: regulation and following of a square wave reference signal, disturbance rejection, and model uncertainty. The regulation and following of the square wave reference signal are examined in Section 5.2.1. The effectiveness of the controller in rejecting different levels of disturbance is evaluated in Section 5.2.2. Moreover, the impact of model uncertainty on the performance of the controller is studied in Section 5.2.3.

#### 5.2.1. Regulating and Following Square Wave

This experiment assesses the efficacy of the LQIR-DG controller in regulating and following a square wave input for the quadrotor's attitude angles. The desired square wave input is generated for the roll and pitch angles, and the quadrotor's response to the input is measured. The results obtained demonstrate the robustness and precision of the LQIR-DG controller in accurately tracking the square wave input.

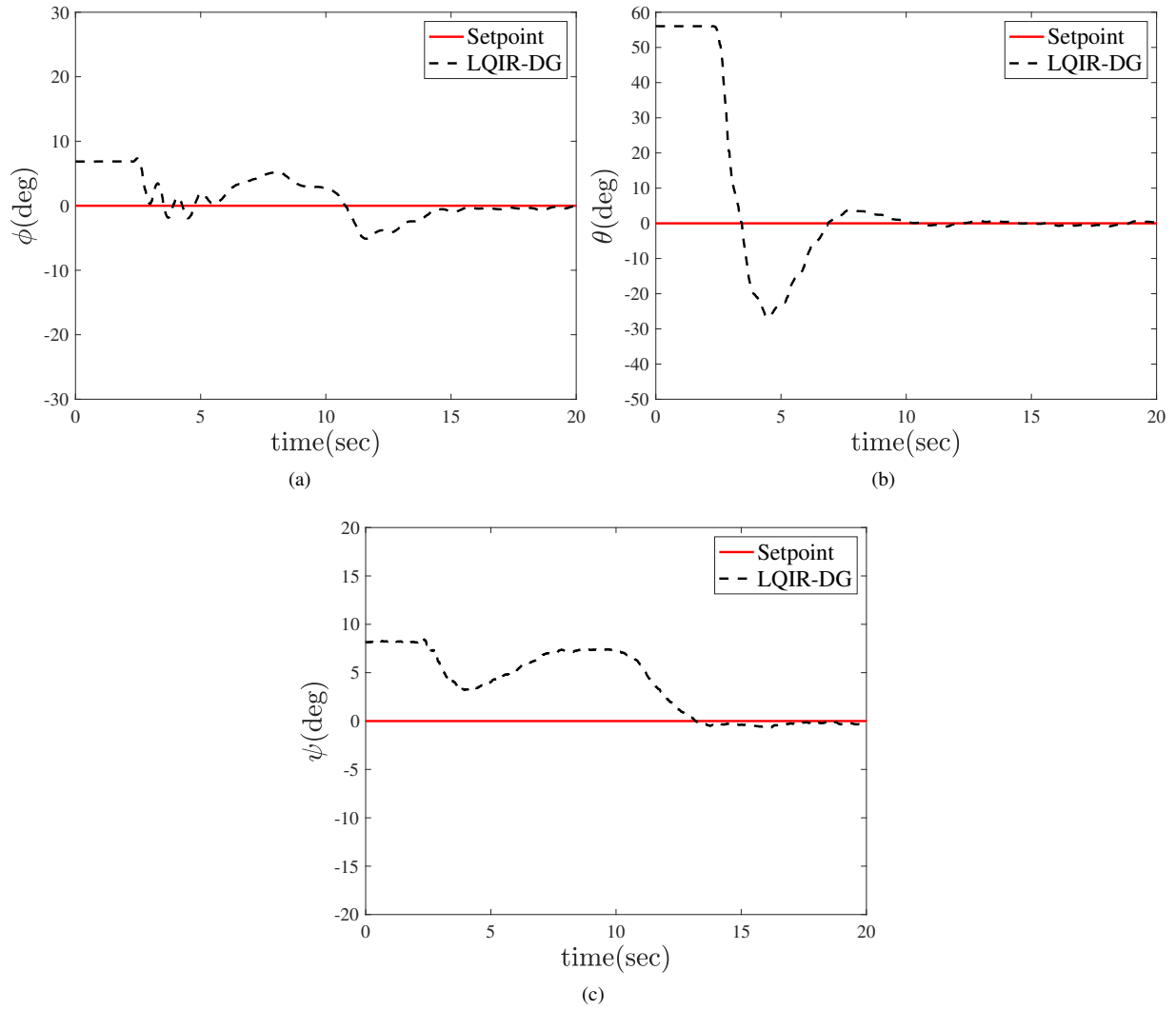


Figure 8: LQIR-DG Controller Efficiency Assessment for Euler Angles Attitude Angles (Roll (a), Pitch (b), and Yaw (c) respectively).

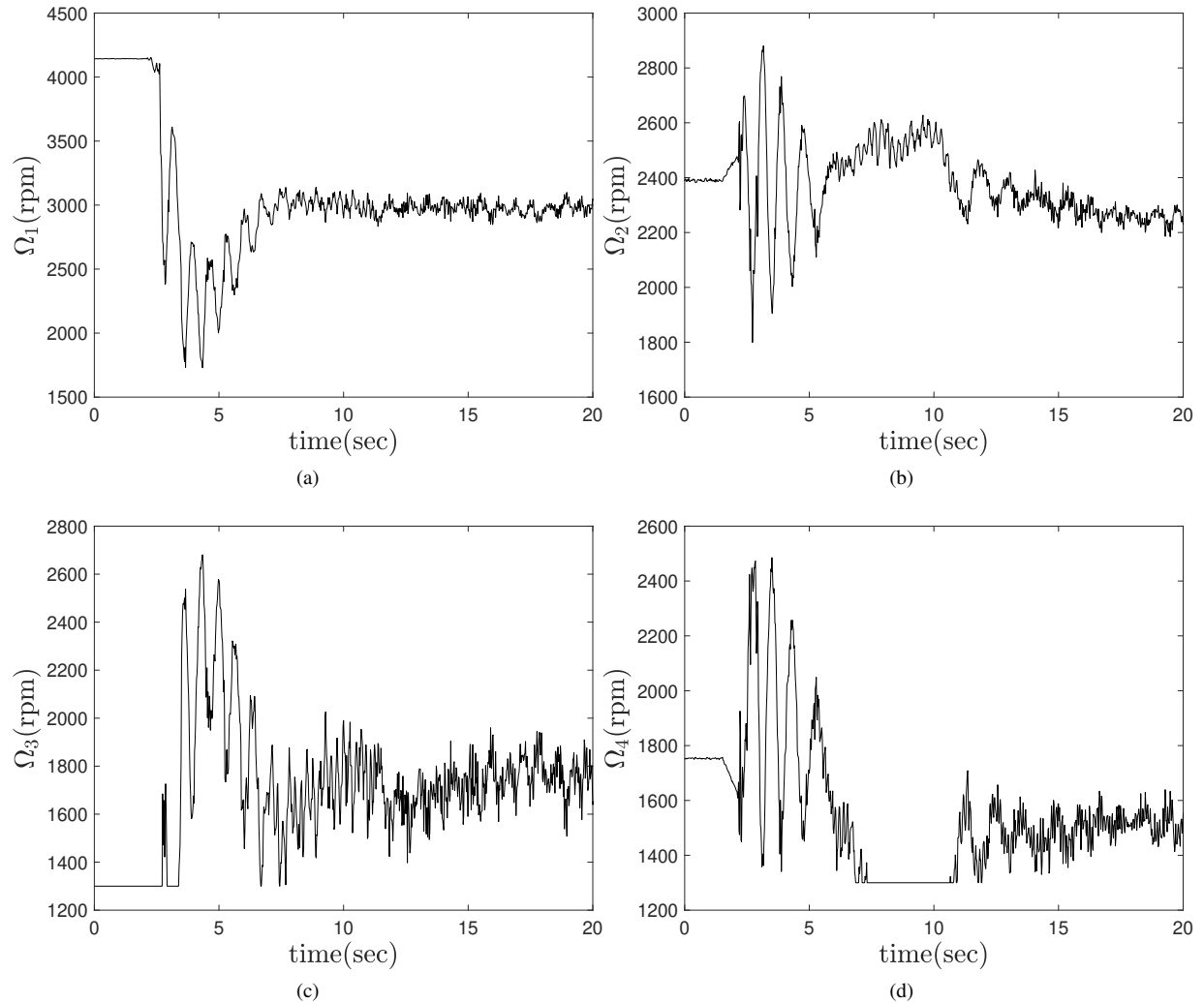


Figure 9: Temporal Evolution of Angular Velocity Commands for the LQIR-DG Controller

Figure 10 The results of this experiment demonstrate the efficacy of the LQIR-DG control strategy in regulating the coupled roll and pitch channels, enabling accurate tracking of a desired square wave input with a frequency of 0.02 Hz and an amplitude of 20 degrees.

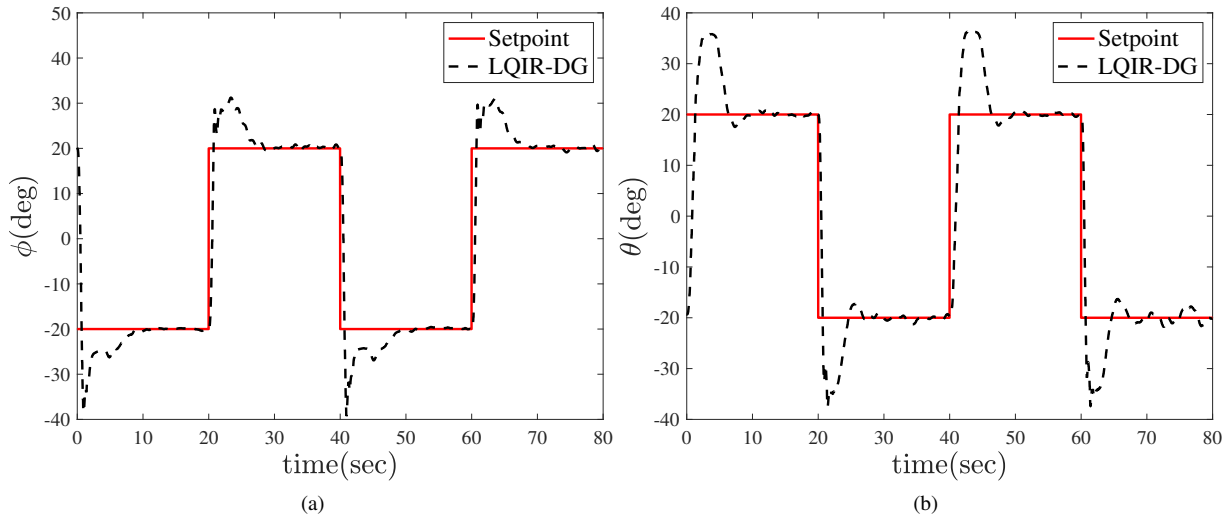


Figure 10: Performance Evaluation of the LQIR-DDG Control Strategy for Tracking Desired Angles in the Two-Degree-of-Freedom Coupling Mode. Subfigure (a) displays the comparison between the actual and desired roll angles, while subfigure (b) shows the comparison between the actual and desired pitch angles.

### 5.2.2. Investigating the possibility of disturbance rejection

This section examines the effectiveness of the LQIR-DG controller in attenuating input disturbances during regulation. To this end, a disturbance with an amplitude of 0.5 N is added to the input signal from 20 to 60 seconds. As depicted in Figure 11, the LQIR-DG controller demonstrates proficient coupling of the roll and screw channels, resulting in effective removal of the input disturbance. Figure 11(a) depicts an evaluation of the controller's performance through a comparison between the desired and actual roll angles, while Figure 11(b) presents a similar analysis for the desired and actual pitch angles. The results indicate that the LQIR-DG controller performs appropriately in mitigating the input disturbance.

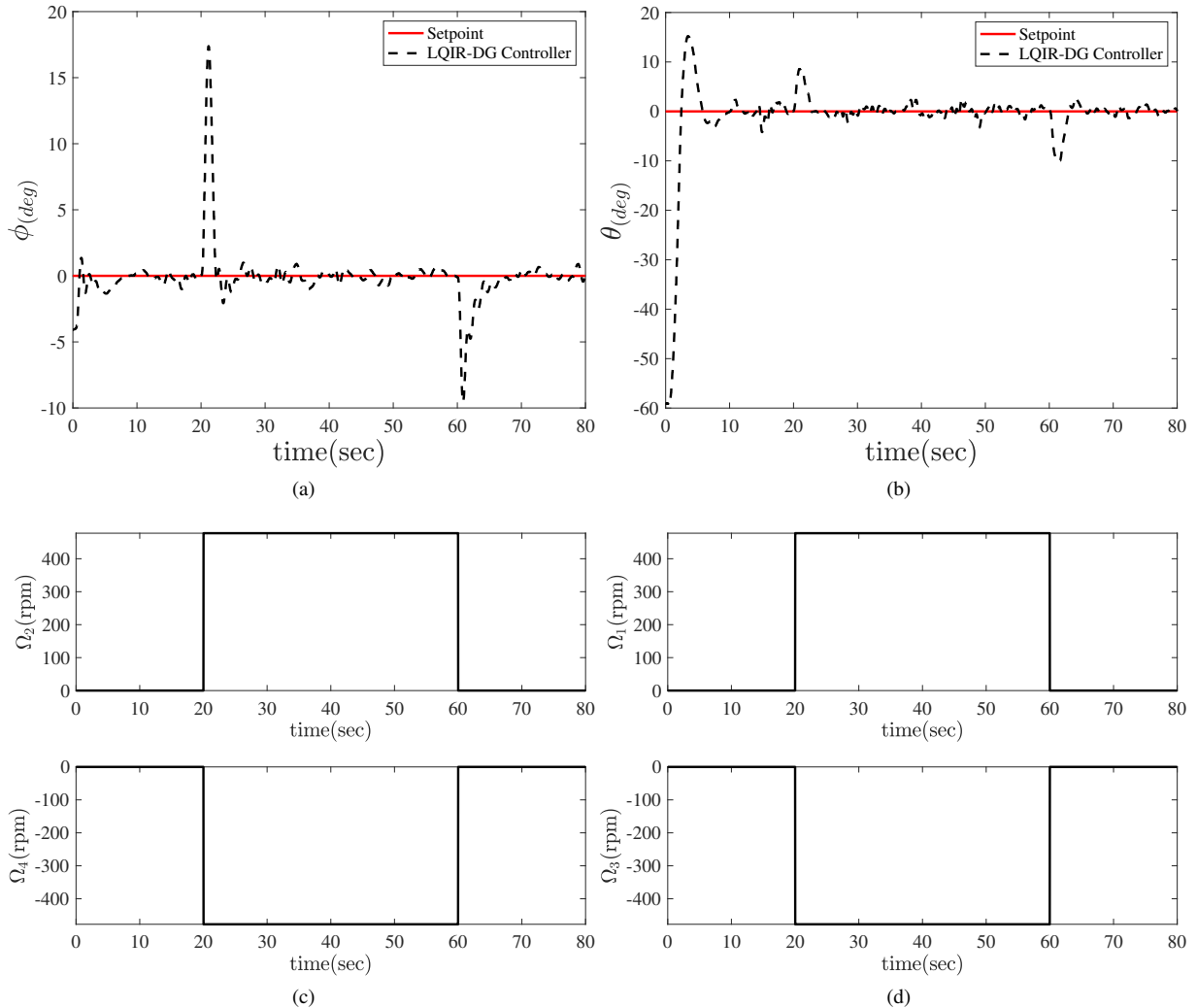


Figure 11: Evaluation of the LQIR-DG control strategy performance under the influence of input disturbance in the two-degree-of-freedom coupling mode. (a) illustrates the comparison between the desired roll angle and the actual value. Similarly, (b) shows the comparison between the desired pitch angle and the actual value.”

### 5.2.3. Investigating the impact of uncertainty in modeling

In this section, the performance of the LQIR-DG controller is investigated under the consideration of uncertainty in the 3DoF experimental setup modeling. Specifically, the controller’s effectiveness in the coupling mode of the roll and pitch channels is evaluated while taking into account the uncertain values of the moments of inertia around each axis of the body coordinate system. The results of this investigation are presented in figure 13, where a disturbance of 50 grams is added to the roll axis and 100 grams to the pitch axis.

Figure 13(a) and (b) depict the evaluation of the LQIR-DG controller with emphasis on the comparison of desired and actual roll and pitch angles, respectively. The implementation results indicate that the LQIR-DG controller performs efficiently in achieving the desired values, even with the uncertainty in the moments of inertia.

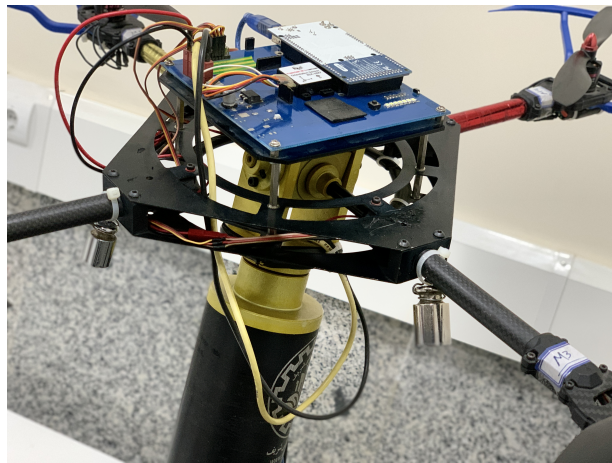


Figure 12: Quadrotor 3DoF Setup with Added Weight.

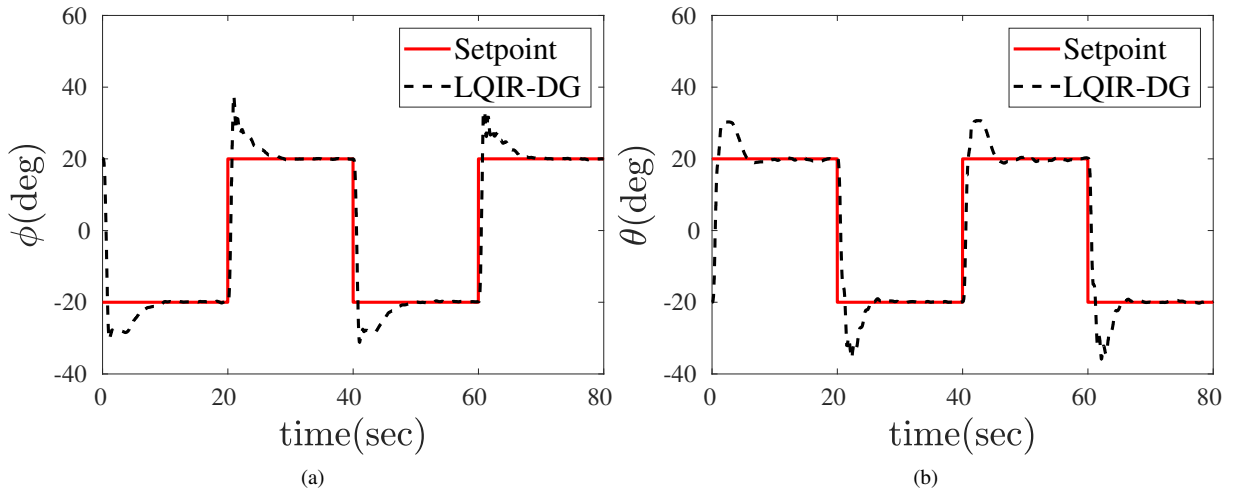


Figure 13: Performance Evaluation of the LQIR-DG Control Strategy under Uncertainty by Weighting Roll and Pitch Axes in Two-Degree-of-Freedom Coupling Mode. Subfigure (a) depicts a comparison of the desired and actual roll angles, while subfigure (b) presents a comparison of the desired and actual pitch angles.

#### 5.2.4. Comparison with LQR, LQIR, and PID

This section compares the implementation performance of three different controllers for the quadrotor system: PID, LQR, and LQIR-DG. The comparison is made based on the implementation results of the controllers in the presence of uncertainty, input disturbance, and weight addition in the two-degree-of-freedom coupling mode.

The PID controller has been widely used in quadrotor control due to its simplicity and ease of implementation. However, its performance is limited in complex scenarios due to the inherent nonlinearity and uncertainty of the quadrotor system.

The LQR and LQIR controller is a linear feedback control method that can provide better performance than PID by optimizing a quadratic cost function. However, it requires an accurate model of the system, and is sensitive to uncertainties and disturbances in the system.

The LQIR-DG controller, which is based on game theory, considers both the system dynamics and the measurement uncertainties, and provides better performance in the presence of uncertainty and disturbances. In addition, the LQIR-DG controller can handle weight additions without requiring a re-design of the controller.

The implementation results indicate that the LQIR-DG controller outperforms the PID and LQR controllers in terms of accuracy and robustness in the presence of uncertainties and disturbances. The comparison results for the three controllers are summarized as follows:

- **PID**

The PID controller can track the desired angles reasonably well in the absence of uncertainties and disturbances. However, its performance is significantly affected by the presence of uncertainty and disturbances, resulting in oscillations and overshoots in the response.

- **LQR and LQIR**

The LQR and LQIR controller provides better performance than PID in the absence of uncertainties and disturbances. However, it is more sensitive to system uncertainties and disturbances, resulting in larger errors and oscillations in the response.

- **LQIR-DG**

Among the three controllers compared, the LQIR-DG controller exhibits superior performance, exhibiting robustness to uncertainties, disturbances, and weight additions without necessitating a re-design of the control system. The LQIR-DG controller provides accurate and robust control of the quadrotor system, with minimal errors and oscillations in the response.

In summary, the LQIR-DG controller provides better performance than PID and LQR controllers, and is a promising control method for quadrotor systems in the presence of uncertainties and disturbances.

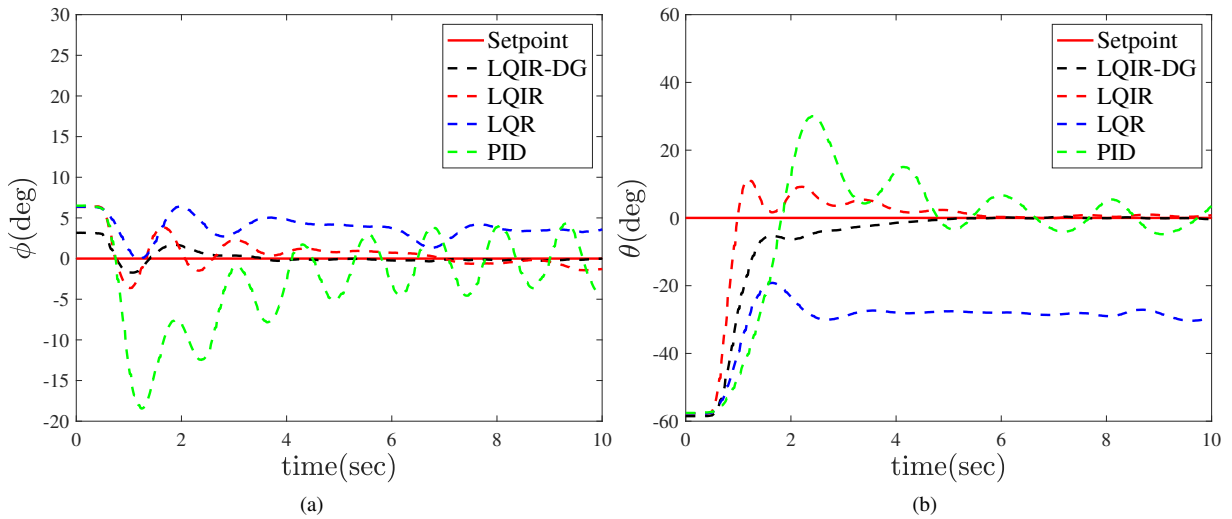


Figure 14: The implementation results of the LQIR-DG Control Strategy with added weight on the roll and pitch axes in the three-degree-of-freedom coupling mode. (a) Comparison of the desired roll angle with the actual roll angle, (b) Comparison of the desired pitch angle with the actual pitch angle.

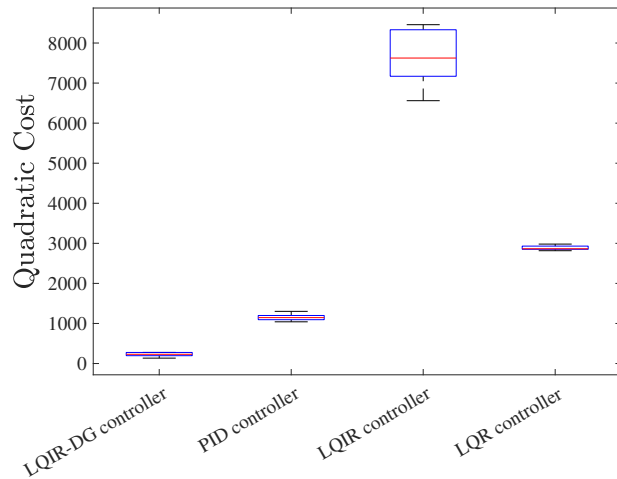


Figure 15: Comparative Analysis of the LQIR-DG Control Strategy versus LQR, LQIR, and PID Controllers using Quadratic Cost Function

## 6. Conclusion

This study has introduced a novel methodology for the implementation and assessment of a controller with integral action utilizing linear quadratic optimization, founded on the principles of differential game theory, with the aim of achieving level attitude control and reference tracking in an experimental platform of the quadrotor. The development of the proposed controller design necessitated the formulation of a precise state-space model for the quadrotor, which was then linearized. The estimation of the model parameters was subsequently conducted in accordance with the design process. The implementation of the LQIR-DG controller required the coordination of two players, with each player dedicated to controlling a specific Euler angle channel. The first player, utilizing a quadratic criterion, performed optimization of the control input for each channel, while another player makes the most challenging disturbances.

The efficacy of the LQIR-DG control strategy was assessed in hover and compared against the PID, LQR, and LQIR controllers. The experimental findings demonstrated the efficacy of the LQIR-DG approach for achieving attitude control, square wave tracking, disturbance rejection, and robustness to model uncertainty in the actual quadrotor platform during level flight. Overall, this study has demonstrated the effectiveness and potential of the LQIR-DG method in quadrotor attitude control, which can be extended to other aerospace systems.

## References

- [1] M. F. Fathoni, S. Lee, Y. Kim, K.-I. Kim, K. H. Kim, Development of multi-quadrotor simulator based on real-time hypervisor systems, *Drones* 5 (3). doi:10.3390/drones5030059.  
URL <https://www.mdpi.com/2504-446X/5/3/59>
- [2] H. Nobahari, A. Sharifi, A hybridization of extended kalman filter and ant colony optimization for state estimation of nonlinear systems, *Applied Soft Computing* 74. doi:10.1016/j.asoc.2018.10.010.
- [3] H. Bolandi, M. Rezaei, R. Mohsenipour, H. Nemati, S. Smailzadeh, Attitude control of a quadrotor with optimized pid controller, *Intelligent Control and Automation* 04 (2013) 342–349. doi:10.4236/ica.2013.43040.
- [4] A. Abdul Salam, I. Ibraheem, Nonlinear pid controller design for a 6-dof uav quadrotor system, *Engineering Science and Technology, an International Journal* 22. doi:10.1016/j.estch.2019.02.005.
- [5] Y. Bouzid, M. Zareb, H. Siguerdidjane, M. Guiatni, Boosting a Reference Model-Based Controller Using Active Disturbance Rejection Principle for 3D Trajectory Tracking of Quadrotors: Experimental Validation, *Journal of Intelligent and Robotic Systems* 100 (2) (2020) 597–614. doi:10.1007/s10846-020-01182-4.  
URL <https://hal.univ-grenoble-alpes.fr/hal-02543214>
- [6] Z. Wang, D. Huang, T. Huang, N. Qin, Active disturbance rejection control for a quadrotor uav, in: 2020 IEEE 9th Data Driven Control and Learning Systems Conference (DDCLS), 2020, pp. 1–5. doi:10.1109/DDCLS49620.2020.9275226.
- [7] C. Nicol, C. Macnab, A. Ramirez-Serrano, Robust neural network control of a quadrotor helicopter, in: 2008 Canadian Conference on Electrical and Computer Engineering, 2008, pp. 001233–001238. doi:10.1109/CCECE.2008.4564736.

- [8] P. Ghiglino, J. L. Forshaw, V. J. Lappas, Online PID Self-Tuning using an Evolutionary Swarm Algorithm with Experimental Quadrotor Flight Results. arXiv:<https://arc.aiaa.org/doi/pdf/10.2514/6.2013-5098>, doi:10.2514/6.2013-5098  
URL <https://arc.aiaa.org/doi/abs/10.2514/6.2013-5098>
- [9] L. V. Nguyen, M. D. Phung, Q. P. Ha, Iterative learning sliding mode control for uav trajectory tracking, *Electronics* 10 (20). doi:10.3390/electronics10202474.  
URL <https://www.mdpi.com/2079-9292/10/20/2474>
- [10] C.-H. Pi, W.-Y. Ye, S. Cheng, Robust quadrotor control through reinforcement learning with disturbance compensation, *Applied Sciences* 11 (7). doi:10.3390/app11073257.  
URL <https://www.mdpi.com/2076-3417/11/7/3257>
- [11] K. Liu, R. Wang, S. Dong, X. Wang, Adaptive fuzzy finite-time attitude controller design for quadrotor uav with external disturbances and uncertain dynamics, in: 2022 8th International Conference on Control, Automation and Robotics (ICCAR), 2022, pp. 363–368. doi:10.1109/ICCAR55106.2022.9782598.
- [12] K. Chara, A. Yassine, F. Srairi, K. Mokhtari, A robust synergetic controller for quadrotor obstacle avoidance using b閦ier curve versus b-spline trajectory generation, *Intelligent Service Robotics* 15. doi:10.1007/s11370-021-00408-0.
- [13] H. Wang, M. Chen, Sliding mode attitude control for a quadrotor micro unmanned aircraft vehicle using disturbance observer, in: Proceedings of 2014 IEEE Chinese Guidance, Navigation and Control Conference, 2014, pp. 568–573. doi:10.1109/CGNCC.2014.7007285.
- [14] A. Aboudonia, A. El-Badawy, R. Rashad, Disturbance observer-based feedback linearization control of an unmanned quadrotor helicopter, *Proceedings of the Institution of Mechanical Engineers Part I Journal of Systems and Control Engineering* 230. doi:10.1177/0959651816656951.
- [15] A. T. Azar, F. E. Serrano, A. Koubaa, N. A. Kamal, Backstepping h-infinity control of unmanned aerial vehicles with time varying disturbances, in: 2020 First International Conference of Smart Systems and Emerging Technologies (SMARTTECH), 2020, pp. 243–248. doi:10.1109/SMART-TECH49988.2020.00061.
- [16] A. Hamza, A. Mohamed, A. El-Badawy, Robust h-infinity control for a quadrotor uav, 2022. doi:10.2514/6.2022-2033.
- [17] W. Dean, B. Ranganathan, I. Penskiy, S. Bergbreiter, J. Humbert, Robust Gust Rejection on a Micro-air Vehicle Using Bio-inspired Sensing, 2017, pp. 351–362.
- [18] E. Barzani, K. Salahshoor, A. Khaki Sedigh, Attitude flight control system design of uav using lqg ltr multivariable control with noise and disturbance, in: 2015 3rd RSI International Conference on Robotics and Mechatronics (ICROM), 2015, pp. 188–193. doi:10.1109/ICRoM.2015.7367782.
- [19] Z. Shulong, A. Honglei, Z. Daibing, S. Lincheng, A new feedback linearization lqr control for attitude of quadrotor, in: 2014 13th International Conference on Control Automation Robotics and Vision (ICARCV), 2014, pp. 1593–1597. doi:10.1109/ICARCV.2014.7064553.
- [20] Z. Zwierzewicz, On the ship course-keeping control system design by using robust and adaptive control, in: 2014 19th International Conference on Methods and Models in Automation and Robotics (MMAR), 2014, pp. 189–194. doi:10.1109/MMAR.2014.6957349.
- [21] Y. Li, L. Guo, Towards a theory of stochastic adaptive differential games, in: 2011 50th IEEE Conference on Decision and Control and European Control Conference, 2011, pp. 5041–5046. doi:10.1109/CDC.2011.6160768.
- [22] S. Bouabdallah, R. Siegwart, Full control of a quadrotor, in: 2007 IEEE/RSJ International Conference on Intelligent Robots and Systems, 2007, pp. 153–158. doi:10.1109/IROS.2007.4399042.
- [23] S. Bouabdallah, Design and control of quadrotors with application to autonomous flyingdoi:10.5075/epfl-thesis-3727.
- [24] J. Engwerda, Linear quadratic games: An overview, Workingpaper, Macroeconomics, subsequently published in *Advances in Dynamic Games and their Applications* (book), 2009 Pagination: 32 (2006).